PCCP

RSC Publishing

PAPER

Recovering degraded quasi-solid-state dye-sensitized solar cells by applying electrical pulses†

Cite this: *Phys. Chem. Chem. Phys.*, 2013, **15**, 6864

Xi Zhang,[a] Xuezhen Huang[a] and Hongrui Jiang*[ab]

Received 14th January 2013,
Accepted 13th March 2013

DOI: 10.1039/c3cp51071a

www.rsc.org/pccp

We discovered a method of applying a forward pulsed bias to recover the degraded quasi-solid-state dye-sensitized solar cells (DSSCs). Up to 30.7% of the power conversion efficiency (η) of a degraded poly(vinylidene fluoride) (PVDF) based DSSC was recovered by a double-pulse. The recovered η remained higher than that before the double-pulse treatment for at least 28 days. It is deduced that the blocking of ion-transport channels in the quasi-solid-state electrolyte causes degradation of the DSSCs. This study will shed light on the efficiency enhancement and long-term stability of quasi-solid-state DSSCs.

1. Introduction

Dye-sensitized solar cells (DSSCs) have attracted tremendous attention in recent years, because of their low cost and high efficiency.[1–3] The DSSCs with highest power conversion efficiency (η) are based on liquid electrolytes, and the recently reported efficiency was over 12%.[4] However, the liquid electrolytes limit the long-term stability of DSSCs. Much effort has been made to replace the liquid electrolytes by solid-state materials, including inorganic hole conductors/p-type semiconductors,[5–7] organic hole conductors,[8–11] nano-composite materials,[12,13] and gel and polymer electrolytes.[14–17] Among these materials, polymer electrolytes have obtained growing interest from the perspective of practical applications owing to their excellent characteristics such as easy fabrication, low cost, good stability and flexibility.[18–20] The stability is a crucial issue for the commercial use of such DSSCs. Nevertheless, very few studies have been reported on the stability and degradation mechanisms of these cells. There is still no report on the recovery of degraded DSSCs. Hence the study of the degradation mechanism and exploring methods to solve the problem are of great significance.

In this study, an appropriate pulsed electrical bias (around 2.5 V) is applied to poly(vinylidene fluoride) (PVDF) based DSSCs to force the redistribution of triiodide (I_3^-) and iodide (I^-) in the electrolyte. Usually such kinds of pulses could cause damage to DSSCs, since a voltage which is much greater than the open-circuit voltage (V_{oc}) could induce a large dark current. Nonetheless, if the pulse width is well controlled, the damage could be avoided. We have found that the efficiency of a degraded solid DSSC could be significantly recovered without causing damage to the cell after applying an appropriate positive double-pulse due to the recovery of the short-circuit photocurrent density (J_{sc}). Such recovery could last in the air in the dark for a long period, at least 28 days. This pulsed-bias method could be practically applied in the actual usage of DSSCs. Furthermore, the recovery of degraded DSSCs by this method also indicates that the blocking of the diffusion of I^-/I_3^- in such a quasi-solid-state electrolyte is a key factor of the degradation mechanism.

2. Experimental

2.1. DSSC fabrication

8 μm-thick TiO_2 films were fabricated on conductive fluorine-doped tin oxide (FTO; resistance: 12–14 Ω per square; transmittance: 82–84%; MTI Co., USA) glass substrates using a screen printing method[21] with a paste consisting of 15–20 nm TiO_2 particles (SOLARONIX, Ti-Nanoxide T/SP, Switzerland). The area of the active region on the FTO glass was 0.12 cm^2. After sintering at 500 °C for 1 h, a 2 μm-thick TiO_2 scattering layer composed of 50–100 nm TiO_2 particles (SOLARONIX, Ti-Nanoxide R/SP, Switzerland) was deposited. The films were subsequently sintered again at 500 °C for 1 h before being dipped into 0.05 M $TiCl_4$ aqueous solution at 70 °C for 30 min, followed by calcination at 450 °C for 30 min to stain the TiO_2 films. The $TiCl_4$-pretreated films were cooled down to 120 °C before being soaked into the dye solutions (0.3 mM N719 in acetonitrile–*tert*-butanol, v/v = 1 : 1) for 24 h. The counter electrode was Pt-coated FTO with two drilled holes for filling the electrolyte. The Pt layer was

[a] *Department of Electrical and Computer Engineering, University of Wisconsin-Madison, Madison, WI 53706, USA. E-mail: hongrui@engr.wisc.edu; Fax: +1 608-262-1267; Tel: +1 608-265-9418*
[b] *Materials Science Program, University of Wisconsin-Madison, Madison, WI 53706, USA*

† Electronic supplementary information (ESI) available. See DOI: 10.1039/c3cp51071a

deposited on the FTO glass by an electrodeposition process in H_2PtCl_6 solution (0.5 M). A 25 μm-thick Surlyn (SOLARONIX, Switzerland) film was used as a spacer between the photoelectrode and the counter electrode for each DSSC. The redox electrolyte contained 0.1 M LiI, 0.05 M I_2, 0.6 M 1,2-dimethyl-3-propylimidazolium iodide, and 2 wt% PVDF (Kynar 301F, M_w = 3.8 × 10^5) using acetonitrile–dimethyl sulfoxide (v/v = 4 : 1) as solvent. The electrolyte solution was repeatedly injected into the space between the photoelectrode and the counter electrode and dried on a hot plate at 40 °C until the porous nano-TiO_2 was fully filled and the solvent was sufficiently removed. Three quasi-solid-state DSSCs were fabricated and tested in this study: C1, C2, and C3. Only for C1, the two holes were sealed with the Surlyn film and a glass slide by heating. C2 and C3 were not sealed to accelerate their degradation.

2.2. Photovoltaic measurement and applying pulses

The current–voltage (*J–V*) measurements of the three DSSCs were performed using a Keithley 2400 source meter under the illumination of simulated AM 1.5G solar light (Oriel 94022A equipped with a 150 W Xe lamp and an AM 1.5G filter). To apply the pulse while retaining the capability to measure the current, we again utilized the Keithley 2400 source meter for the electrical pulses. The source meter was controlled by a computer program to generate pulses with a constant 185 ms width. The shapes of the output pulses were recorded using an Agilent DSO5014A oscilloscope.

2.3. Characterization and stability tests

The morphology of the nano-TiO_2 photoelectrode covered by the gel electrolyte was characterized by using a scanning electron microscope (SEM, Zeiss LEO 1530). The transient photocurrent curves were recorded using an Agilent 34411A $6_{1/2}$ digital multimeter. The electrochemical impedance spectroscopy (EIS) was carried out using an SP-200 potentiostat (Biologic, USA), with the frequency ranging from 100 Hz to 200 kHz. The DSSCs were kept at open circuit potentials under AM 1.5G illumination for the EIS test. For the long-term stability tests, *J–V* curves of C1 and C3 under AM 1.5G illumination were recorded intermittently for a long period. When C1 and C2 were not tested, they were kept in the air in the dark, at 25 °C temperature and 30% humidity.

3. Method and mechanism

When a positive pulsed electrical bias (counter electrode with positive potential, photoelectrode with zero potential) is applied to a DSSC, electrons are injected from the conduction band of the TiO_2 photoelectrode to the redox level of the electrolyte.[22] The following reaction then occurs at the TiO_2/dye/electrolyte interface:

$$I_3^- + 2e\ (TiO_2) \rightarrow 3I^-, \quad (1)$$

where plenty of I^- ions are produced near this interface. Meanwhile, I_3^- ions in the same amount are produced near the counter electrode *via* a reverse reaction of eqn (1), as shown in Fig. 1. The net effect of the positive pulse is therefore the increased concentration of I^- near the TiO_2 photoelectrode, while the concentration of I_3^- near the counter electrode is increased. After the pulse, the concentration gradient drives the ions to diffuse back to the initial equilibrium.

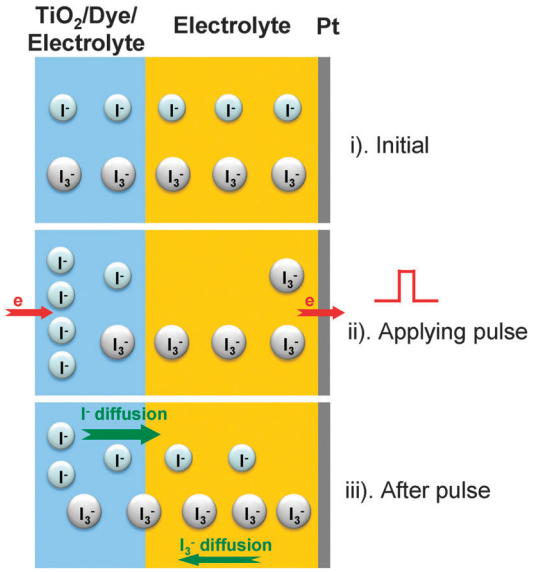

Fig. 1 Schematic of the ion distribution in the electrolyte before and after the application of the positive pulse in a typical DSSC. The region on the left represents the dye-loaded TiO_2 nanoparticles surrounded by the electrolyte, while the middle region between the TiO_2 photoelectrode and the Pt counter electrolyte represents the pure electrolyte.

When DSSCs operate under illumination, the I^- ions near the photoelectrode provide the electrons to the lowest unoccupied molecular orbital (LUMO) energy level of the dye to contribute to the photocurrent. For typical liquid electrolytes with a high conductivity, the concentration of I^- does not influence the photocurrent of the DSSCs. However for quasi-solid-state and other viscous electrolytes, their diffusion coefficients are too low to maintain a sufficiently large flux of I^-/I_3^- transport, which limits the photocurrent.[23] The photocurrent of a quasi-solid-state DSSC increases with I^-/I_3^- concentration.[24,25] Therefore, the immediate J_{sc} of a quasi-solid-state DSSC after the positive pulse should be improved if the pulse does not bring any damage to the cell. Afterwards, the electrolyte will return to the initial equilibrium, and J_{sc} should drop back to the initial value before the pulse.

As shown in Fig. 2a, the PVDF-based electrolyte covers the TiO_2 nanoparticles and fills in their interspace. In such a quasi-solid-state polymer electrolyte, framework materials provide the liquid-like channels for the transport of I^-/I_3^-.[23,26] If a DSSC is degraded by the blockage of such channels, the large transient current during the pulse may open up some of them to recover the performance, as shown in Fig. 2c. If this hypothesis is true, the performance of the DSSC should still be better when reaching the equilibrium after a pulse period, compared with that before the pulse.

To set the parameters of the pulse in the experiments, the total quantity of I atoms in the electrolyte should be considered, according to eqn (1). The number of the injected electrons

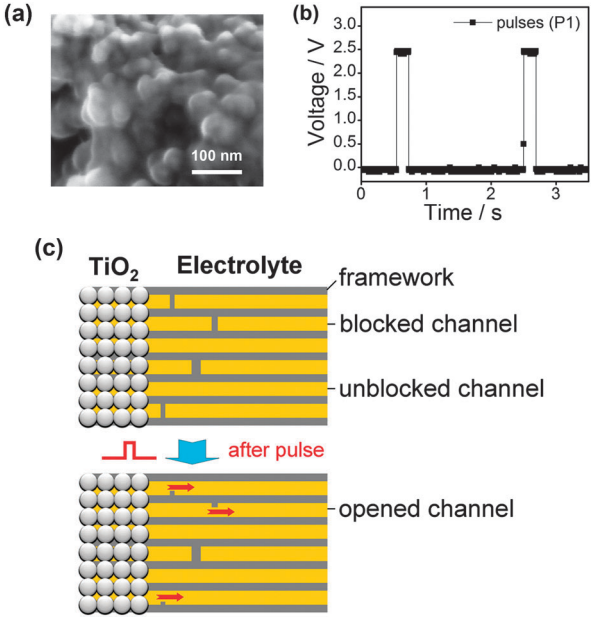

Fig. 2 (a) SEM image of the nano-TiO_2 photoelectrode covered by the gel electrolyte. (b) Double 185 ms electrical pulses (P1) generated using the source meter, measured using an oscilloscope. (c) Some of the blocked ion-transport channels in this quasi-solid-state electrolyte are opened up by the applied pulse.

via the pulse should be fewer than or at most comparable with the total number of I atoms in the electrolyte. If the injected electrons significantly outnumbers the I atoms, the excessive electrons may cause some irreversible damage to the cell. Hence the control of the parameters of the pulse is crucial. In our experiments, the basic pulse parameters are shown in Fig. 2b, with a constant 185 ms pulse width. During the pulse period, the currents near the rising and falling edges were recorded, respectively, typically around 40–45 mA for C1, C2, and C3 with 2.5 V pulse height. Using an average current of 40 mA, the total number of injected electrons (N_{inj}) can be estimated to be 4.6×10^{16}. The total number of I atoms in the electrolyte (N_I) can be calculated to be 1.4×10^{16}, with $[I_2]$ = 0.05 M and an estimation of 50% porosity of TiO_2 films. Thus N_{inj} is sufficient and relatively comparable with N_I.

4. Results and discussion

In the first study, two single 185 ms pulses separated by 2 s were applied to enhance the pulse effect. The measured double-pulse with 2.5 V in height is shown in Fig. 2b, called P1. The transient currents at the beginning and the end of the pulse applied to the DSSC were recorded using the Keithley 2400 source meter. For C1, the average current under the 2.5 V pulse was measured to be about 40 mA. *J–V* curves of C1 before and after P1 are shown in Fig. 3a. The *J–V* curve of C1 before P1 was first recorded. After P1, *J–V* was recorded immediately (2 s after P1), showing a great improvement in J_{sc} by about 25%. However, the *J–V* curve at the low voltage region is a little steep, indicating a nonequilibrium state of the cell. After 2 min, *J–V* was recorded again (also in Fig. 3a), showing a decreased but flatter photocurrent.

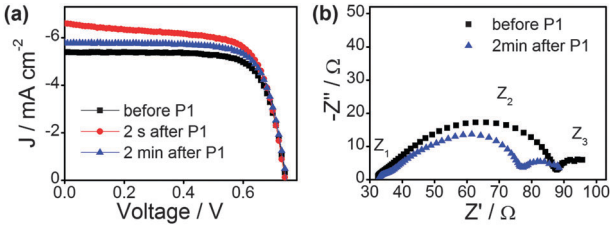

Fig. 3 (a) *J–V* curves under AM 1.5G and (b) Nyquist plots of C1 before and after P1. EIS measurements were performed under AM 1.5G illumination and with +0.74 V bias on C1 (open-circuit).

This is due to the diffusion of I^-/I_3^- as shown in Fig. 1. Here, J_{sc} of C1 is still greater than that before P1. V_{oc} was not affected by the pulses during the process.

In order to understand the mechanism of the increase in the photocurrent, EIS under AM 1.5G illumination at open-circuit potentials was performed, and the Nyquist plots of C1 before and after P1 are shown in Fig. 3b. The three semi-circles in each curve refer to the impedances at the Pt electrode (Z_1), the TiO_2/dye/electrolyte interface (Z_2), and in the electrolyte (Z_3), respectively.[27,28] Simulation of the two spectra in Fig. 3b was performed using a Z-View software, and all the impedances were obtained, shown in Fig. S1 and Table S1 (ESI†). After P1, Z_2 was greatly reduced, indicating that the conductivity at the TiO_2/dye/electrolyte interface was greatly improved. This result confirms the increase in the I^- concentration at the TiO_2/dye/electrolyte interface by the pulses, as previously discussed. The change in Z_1 and Z_3 induced by P1, on the other hand, is not remarkable. The series resistances of the two curves, located at about 33 Ω, were almost unchanged either. Therefore, the region acted upon by the pulses in the DSSC is essentially at the TiO_2/dye/electrolyte interface.

C2 was tested to investigate the impact of the pulse height by varying the pulse height. Three double-pulses with pulse heights of 2.5 V (P1), 2.8 V (P2), and 3.2 V (P3) were applied to C2 in sequence and the photocurrent after applying each of them was measured, as shown in Fig. 4. C2 was kept in the dark initially. When the AM 1.5G radiation was turned on, the photocurrent dropped quickly in tens of seconds to a stable state and flattened. The measured J_{sc} corresponded to the flat photocurrent. The light was shut down after about 250 s, when P1 was applied to C1, before the light was turned on again. Both the initial and the stable photocurrents were improved, respectively, from before the pulse was applied. Similar procedures were followed before applying P2 and P3. After P2, the photocurrent was further improved, where the average transient current induced by 2.8 V pulses in the dark was up to 55 mA. After P3, the improvement of photocurrent was even greater: the initial photocurrent was over 2 mA (17 mA cm^{-2}), and the stable current was 1.2 mA (10 mA cm^{-2}). With the height of the double-pulse increased from 2.5 V to 3.2 V, the pulse-induced dark current in C2 increased from 45 mA to 68 mA correspondingly. This experiment shows that the higher the pulse height, the larger the photocurrent.

As to the impact of the pulse height on η, *J–V* was measured before and after the three double-pulses, and the performance parameters are shown in Table S2 (ESI†). Several minutes

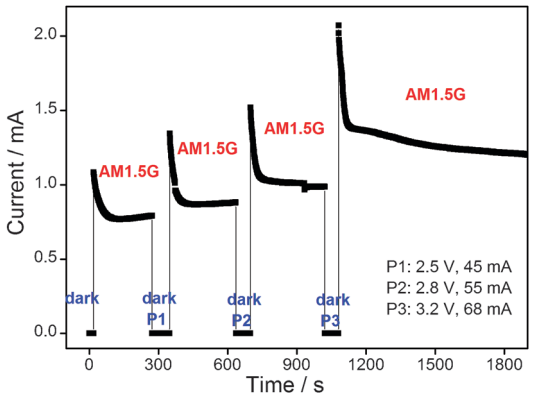

Fig. 4 Transient photocurrent curves of C2 under AM 1.5G illumination: before and after +2.5 V (P1), +2.8 V (P2), and +3.2 V (P3) double-pulses. The average dark currents induced by each pulse are also shown.

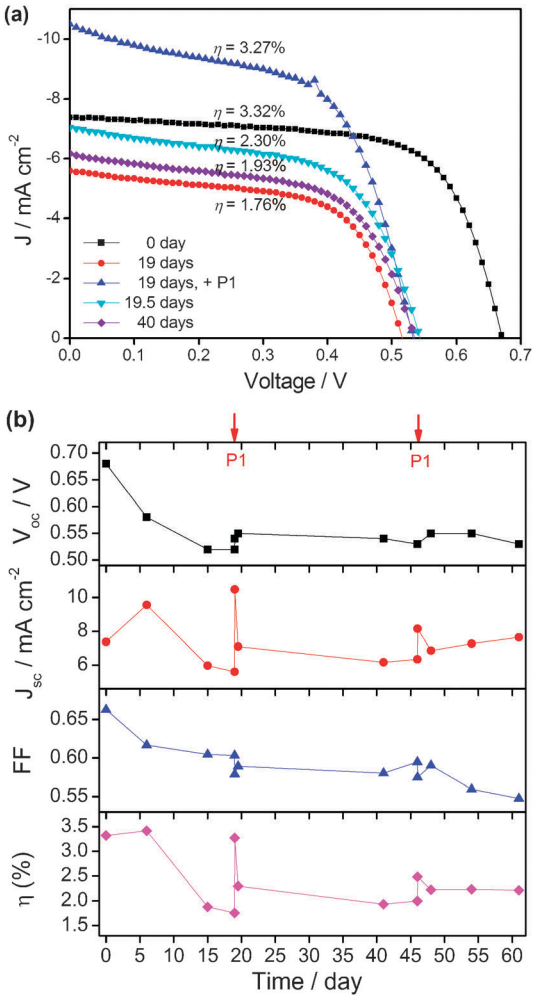

Fig. 5 (a) Measured *J–V* curves of C3 during the first 40 days. The holes on the counter electrode of C3 were not sealed. (b) The corresponding evaluation of the four photovoltaic performance parameters for 61 days, during which the pulses were applied twice: on the 19th day and 46th day, respectively.

after P3, η decreased from 1.90% to 1.83%. Therefore, C2 was partially damaged after P1 to P3. After several days, C2 was severely damaged with η dropping close to 0. The tests carried out on C2 show that higher pulses such as P3 could cause irreversible damage. For our DSSCs, the dark current during each pulse was controlled to be below 50 mA by adjusting the pulse height.

To study the long-term stability of such DSSCs, the *J–V* curves of C1 and C3 during a long period were recorded. It is well known that quasi-solid-state DSSCs have a great stability.[29,30] In our study, the well-sealed C1 kept stable for at least 147 days, as shown in Fig. S2 (ESI†). It was thus difficult to observe any recovery effect by the pulses. On the other hand, the result implies that the applied pulses did not deteriorate the performance of C1. The result of C3 is shown in Fig. 5. Since the holes on the counter electrode were not sealed, C3 degraded rapidly during the first 19 days – all the 4 parameters in Fig. 5b kept dropping from the 5th day to the 19th day. After 19 days, η of C3 dropped from 3.32% to 1.76%, indicating a loss of 47.0% in η due to degradation. On the 19th day, P1 was applied to C3. Then a *J–V* measurement was immediately performed. Similar to the case of C1, there was a great improvement in J_{sc}, which increased η to 3.27%. Meanwhile, V_{oc} increased slightly and the fill factor (FF) dropped slightly. After a half day when C3 reached a stable state, η dropped to 2.30%. This corresponds to a 30.7% of recovery as compared to the degraded η, or a 16.3% of the initial value of η of the fresh C3. Then after another 22 days, η dropped slowly to 1.93%, still greater than the value before applying P1 (1.76%). These results are consistent with our previous hypotheses: first, the channel-blocking effect is an important degradation mechanism in such quasi-solid-state DSSCs, since it could be recovered by the pulse method; second, the well-controlled electrical pulses do not damage the DSSCs. Therefore this pulse method is an effective tool to recover the degraded quasi-solid-state DSSCs. In such PVDF-based DSSCs, the electrolyte conducts by the movement of I^-/I_3^- ions through the matrix channels formed by PVDF. One of the probable degradation reasons of such DSSCs is that some of the ion transport channels are blocked. During the pulse period, part of the blocked channels may be opened up by the large current of I^-/I_3^- ions enforced by the electrical field.

On the 46th day, the same double-pulse was applied to C3 again, and a similar effect was observed: η increased and remained stable for the following 15 days. Such repeatability further proves the significance of this pulse method for recovering the degraded quasi-solid-state DSSCs. The success of P1 for C3 further shows that well-controlled pulse height would not damage the cell. During all the 61 days of test shown in Fig. 5b, FF, kept dropping gradually, and the applied pulses had no positive effect on it. V_{oc} and J_{sc} could be improved by the pulses, and the tendency of η was primarily attributed to J_{sc}, since the change in V_{oc} was not significant. Overall, η was partially recovered.

The degradation of dyes is a key factor influencing the stability of DSSCs.[31–35] Usually such degradation is active when DSSCs are illuminated and/or heated (typically above 60 °C). In our study of long-term stability, the DSSCs were mostly kept in the dark at room temperature except during testing. Therefore this dye degradation should be limited in our study. The degradation of the Pt counter electrode could also be another factor.[36–38] However, the pulse method in this study does not

have any recovery effect on this kind of degradation. Self-degradation in quasi-solid-state DSSCs has been reported due to shrinkage of the polymer electrolytes under a high-humidity atmosphere.[39] The applied pulses could not effectively repair the shrinkage, and the humidity in our study was not too high. No obvious shrinkage was observed in our degraded cells. Nonetheless, the moisture could be one probable factor that acts onto the inside of the ion-channels and causes the blocking. More future work is still needed to verify the details in the channel-blocking process.

5. Conclusion

In conclusion, we have found that applying forward pulsed biases could effectively recover the degradation of quasi-solid-state DSSCs. In a long-term *J–V* measurement, up to 30.7% of the degraded η was recovered by a well-controlled double-pulse. The recovery by the application of the pulses could last more than 28 days. It is believed that the blockage of the ion-transport channel at the interface of TiO_2/dye/electrolyte is an important factor that causes the degradation, and the applied pulses could open the blockage to recover the degraded DSSCs. The recovery of η is mainly from the improvement in the photocurrent, which could be greatly improved when the height of the applied double-pulse increases. However, the height of the double-pulse needs to be well controlled, since the DSSCs might be damaged if the pulse-induced dark current is too large. This finding provides not only a practical method to recover the degraded quasi-solid-state DSSCs, but also an effective tool to study their degradation mechanism. In the future, the long-term stability of the well-sealed quasi-solid-state DSSCs and their degradation mechanism, as well as this approach of ours using forward biased pulses to recover the degraded η, will be further investigated.

Acknowledgements

This work was supported by the US National Institute of Health (Grant No. 1DP2OD008678-01). The authors thank B. Aldalali for assistance in fabricating the printing screen, and Prof. S. Jin and Dr L. Li for EIS measurements. This research utilized US National Science Foundation supported shared facilities at the University of Wisconsin.

Notes and references

1 B. O'Regan and M. Grätzel, *Nature*, 1991, **353**, 737.
2 Y. Chiba, A. Islam, Y. Watanabe, R. Komiya, N. Koide and L. Han, *Jpn. J. Appl. Phys.*, 2006, **45**, L638.
3 Q. Yu, Y. Wang, Z. Yi, N. Zu, J. Zhang, M. Zhang and P. Wang, *ACS Nano*, 2010, **4**, 6032.
4 A. Yella, H. W. Lee, H. N. Tsao, C. Yi, A. K. Chandiran, M. K. Nazeeruddin, E. W. G. Diau, C. Y. Yeh, S. M. Zakeeruddin and M. Grätzel, *Science*, 2011, **334**, 629.
5 K. Tennakone, V. Perera, I. Kottegoda and G. Kumara, *J. Phys. D: Appl. Phys.*, 1999, **32**, 374.
6 Q. B. Meng, K. Takahashi, X. T. Zhang, I. Sutanto, T. N. Rao, O. Sato and A. Fujishima, *Langmuir*, 2003, **19**, 3572.
7 I. Chung, B. Lee, J. He, R. P. H. Chang and M. G. Kanatzidis, *Nature*, 2012, **485**, 486.
8 U. Bach, D. Lupo, P. Comte, J. E. Moser, F. Weissortel, J. Salbeck, H. Spreitzer and M. Grätzel, *Nature*, 1998, **395**, 583.
9 Y. Saito, N. Fukuri, R. Senadeera, T. Kitamura, Y. Wada and S. Yanagida, *Electrochem. Commun.*, 2004, **6**, 71.
10 N. Hirata, J. E. Kroeze, T. Park, D. Jones, S. A. Haque, A. B. Holmes and J. R. Durrant, *Chem. Commun.*, 2006, 535.
11 H. Wang, X. Zhang, F. Gong, G. Zhou and Z.-S. Wang, *Adv. Mater.*, 2012, **24**, 121.
12 T. Stergiopoulos, I. M. Arabatzis, G. Katsaros and P. Falaras, *Nano Lett.*, 2002, **2**, 1259.
13 M. Kaneko and T. Hoshi, *Chem. Lett.*, 2003, 872.
14 L. Wang, S. Fang, Y. Lin, X. Zhou and M. Li, *Chem. Commun.*, 2005, 5687.
15 P. Wang, S. M. Zakeeruddin, J. E. Moser, M. K. Nazeeruddin, T. Sekiguchi and M. Grätzel, *Nat. Mater.*, 2003, **2**, 402.
16 T. Stergiopoulos, I. M. Arabatzis, G. Katsaros and P. Falaras, *Nano Lett.*, 2002, **2**, 1259.
17 J. H. Kim, M. S. Kang, Y. J. Kim, J. Won, N. G. Park and Y. S. Kang, *Chem. Commun.*, 2004, 1662.
18 J. H. Wu, S. C. Hao, Z. Lan, J. M. Lin, M. L. Huang, Y. F. Huang, L. Q. Fang, S. Yin and T. Sato, *Adv. Funct. Mater.*, 2007, **17**, 2645.
19 Q. Li, J. Wu, Z. Tang, Y. Xiao, M. Huang and J. Lin, *Electrochim. Acta*, 2010, **55**, 2777.
20 K. Fan, T. Peng, J. Chen, X. Zhang and R. Li, *J. Mater. Chem.*, 2012, **22**, 16121.
21 Z.-S. Wang, H. Kawauchi, T. Kashima and H. Arakawa, *Coord. Chem. Rev.*, 2004, **248**, 1381.
22 K. Zhu, S. R. Jang and A. J. Frank, *J. Phys. Chem. Lett.*, 2011, **2**, 1070.
23 A. Hagfeldt, G. Boschloo, L. Sun, L. Kloo and H. Pettersson, *Chem. Rev.*, 2010, **110**, 6595.
24 W. Kubo, K. Murakoshi, T. Kitamura, S. Yoshida, M. Haruki, K. Hanabusa, H. Shirai, Y. Wada and S. Yanagida, *J. Phys. Chem. B*, 2001, **105**, 12809.
25 M. Y. Li, S. J. Feng, S. B. Fang, X. R. Xiao, X. P. Li, X. M. Zhou and Y. Lin, *Electrochim. Acta*, 2007, **52**, 4858.
26 Y. Yang, C. H. Zhou, S. Xu, H. Hu, B. L. Chen, J. Zhang, S. J. Wu, W. Liu and X. Z. Zhao, *J. Power Sources*, 2008, **185**, 1492.
27 L. Y. Han, A. Fukui, Y. Chiba, A. Islam, R. Komiya, N. Fuke, N. Koide, R. Yamanaka and M. Shimizu, *Appl. Phys. Lett.*, 2004, **84**, 2433.
28 Q. Wang, J. E. Moser and M. Grätzel, *J. Phys. Chem. B*, 2005, **109**, 14945.
29 Z. Yu, D. Qin, Y. Zhang, H. Sun, Y. Luo, Q. Meng and D. Li, *Energy Environ. Sci.*, 2011, **4**, 1298.
30 Q. Yu, C. Yu, F. Guo, J. Wang, S. Jiao, S. Gao, H. Li and L. Zhao, *Energy Environ. Sci.*, 2012, **5**, 6151.
31 H. G. Agrell, J. Lindgren and A. Hagfeldt, *Sol. Energy*, 2003, **75**, 169.

32 H. Tanaka, A. Takeichi, K. Higuchi, T. Motohiro, M. Takata, N. Hirota, J. Nakajima and T. Toyoda, *Sol. Energy Mater. Sol. Cells*, 2009, **93**, 1143.
33 L. Ke, S. B. Dolmanan, L. Shen, P. K. Pallathadk, Z. Zhang, D. M. Y. Lai and H. Liu, *Sol. Energy Mater. Sol. Cells*, 2010, **94**, 323.
34 M. Natalia and T. Alessandro, *Energy Environ. Sci.*, 2011, **4**, 4473.
35 C. Yoshida, S. Nakajima, Y. Shoji, E. Itoh, K. Momiyama, K. Kanomata and F. Hirose, *J. Electrochem. Soc.*, 2012, **159**, H881.
36 C.-H. Lee, K.-M. Lee, Y.-L. Tung and J.-M. Wu, *J. Electrochem. Soc.*, 2012, **159**, B430.
37 G. Xue, Y. Guo, T. Yu, J. Guan, X. Yu, J. Zhang, J. Liu and Z. Zou, *Int. J. Electrochem. Sci.*, 2012, **7**, 1496.
38 G. Syrrokostas, A. Siokou, G. Leftheriotis and P. Yianoulis, *Sol. Energy Mater. Sol. Cells*, 2012, **103**, 119.
39 J. Y. Lee, B. Bhattacharya, Y. H. Kim, H.-T. Jung and J.-K. Park, *Solid State Commun.*, 2009, **49**, 307.